STUDY ON FINITE ELEMENT METHOD COUPLED WITH GENETIC ALGORITHM IN OPTIMIZATION FOR TEMPERATURE UNIFORMITY OF HOT PLATE WELDING

Cheng Wang[1*] Kaixiang Chang[1] Xiang Liu[1] Weixin Shi[1] Senhui Wang[1*]

[1] *School of Mechatronics Engineering, Anhui University of Science and Technology, Huainan 232001, China.*

* Correspondence author: Cheng Wang: *aust_wangch@163.com*;
Senhui Wang: *wangsenhui613@163.com*.

Abstract

Aiming to improve the temperature uniformity used for hot plate welding, two optimal design methods by coupling finite element method (FEM) with genetic algorithm (GA) are put forward and implemented into FEM software through the secondary development. Taking the positions of the heating holes and the heat fluxes applying to the heating holes as the optimization variables, the minimum temperature difference on the faying surface as the optimization objective, taking advantage of the numerical calculation of steady-state heat transfer, the parametric modeling of hot plate is carried out in accordance with the developed FEM-GA coupling optimization framework. The first optimal design method adopts a two-stage sequent optimization that the optimal positions of heating holes and the heat fluxes applying to the heating holes are sequentially obtained by using the two-step FEM-GA coupling calculations. The second optimal design method optimizes these variables simultaneously. The simultaneous optimal design method is further utilized to optimize the hot plate model associated with the orthogonal heating holes. In the case of the experience-based initialization of the optimization parameters, the two-stage sequent optimal design method is capable to achieve the better temperature uniformity on the faying surfaces with the lower computation costs, as compared with the results of the simultaneous optimal design method. The FEM-GA coupling optimal design method for improving the temperature uniformity used for hot plate welding would be of great significance for the industrial application of hot plate welding.

Key words: *Temperature uniformity; hot plate welding; genetic algorithm; finite element method.*

1. Introduction

Owing to the distinct advantages, such as the good thermal and electrical insulation properties, corrosion resistance, chemical inertness, high strength-to-weight ratio, the application and demand of plastics products are increasing day by day. In the processing of plastic products, the plastic welding is one of the most important technologies, which plays a decisive role in the service performance of plastic products. In general, the approaches widely-used for joining plastics components could be divided into three major categories: the mechanical joining [1, 2], adhesive bonding [3, 4] and welding or fusion bonding [5]. In comparison with the mechanical joining and adhesive bonding, the welding or fusion bonding has the advantages of the higher mechanical strength, better sealing and longer working life. The welding process is frequently used for the thermoplastics, and the addition of tie-layers should be utilized

for welding of the thermosets.

With the rapid development of numerical computation and optimization algorithms, a large number of researches have been reported on the optimization of the temperature uniformity of heated tools used for joining plastics. Ulker et al. [6, 7] took advantage of Taguchi method for investigating the influence of welding parameters in hot plate welding process of polycarbonate/acrylonitrile-butadiene-styrene blends, and the optimization in terms of plate temperature, heating time and welding displacement was accordingly carried out for the improvement of joint strength. Wang et al. [8] developed a multi-objective optimization method by integrating the response surface methodology and the multi-objective particle swarm optimization algorithm for the optimization design of the heating/cooling channels of the steam-heating PTR mold to improve the thermal efficiency and temperature uniformity of the rapid heat cycle molding (RHCM) mold. Chen et al. [9, 10] proposed a variable mold temperature method by controlling the electromagnetic induction heating and water cooling during the microcellular foam injection molding process for improving the surface quality of molded parts. Lambiase et al. [11, 12] developed a 3D finite element model to predict the thermal field induced by Laser-Direct Joining, the influence of the processing conditions including laser beam power, laser energy, laser beam position and beam defusing on the temperature field produced at the interface in metal-polymer joints was investigated, and the optimization of laser-assisted joining of metals and plastics was carried out accordingly. Yildizeli et al. [13] used a multi objective genetic optimization (NSGA-II in MATLAB) to find the optimal operating and geometric design parameter sets for achieving the remarkable improvements in terms of the hydrodynamic and thermal performances of the micro-channel heat sink based on numerical simulation.

Especially for the hot plate welding, Novakovic et al. [14] used the support vector machines and regression models to developed the new mathematical models for providing a visual representation of high-density polyethylene melt displacement with the changes in temperature and pressure. Mathiyazhagan et al. [15] adopted Decision Making Trial and Evaluation Laboratory (DEMATEL) to study the influence of the key parameters including the hot plate temperature, welding time and melting time on the weld strength. Wałęsa et al. [16, 17] developed and constructed a drive system of an automated hot plate welder, the technological parameters were optimized by using the genetic algorithm, and the topic of butt welding of polyurethane drive belts by the hot plate welder was discussed. Riahi et al. [18] studied the plasticization of polyethylene by analytical and numerical methods. He tried to find the correlation between the strength of the joint and welding time or hot plate temperature.

In recent years, with the rapid development of finite element method (FEM) and genetic algorithm (GA), an innovative optimal design method coupling FEM with GA has emerged and became increasingly popular in optimization of welding parameters, machining parameters and heat conduction analysis. In the FEM-GA coupling optimization framework, FEM provides the accurate physical modeling, while GA searches for optimal solutions [19, 20]. Guillaume Corriveau et al. [21] developed an FEM-GA coupling model to automate optimization of static criteria for achieving efficient solutions without engineer intervention. Abdelkader Kanssab et al. [22] took advantage of FEM-GA coupling optimal design for optimizing throat positions and dimensions to achieve a uniform temperature distribution on the pan bottom of an inductor with four throats. Ya Ge et al. [23] utilized FEM with GA and particle swarm optimization to maximize the output power of variable cross-section thermoelectric generators by optimizing six geometric variables and external load resistance.

Although extensive research has been conducted on the optimization of the processing parameters of the plastics welding methods, there are few reports on the temperature uniformity on the faying surfaces used in the hot plate welding of plastics, which has a significant impact on the plastics welding quality.

Therefore, this work devotes to optimizing the positions of heating holes and the related heat fluxes appling to the heating holes by coupling finite element method (FEM) with the genetic algorithm (GA), for achieving the excellent temperature uniformity on the faying surface used in the hot plate welding, which is of great significance for the development of the plastics processing technology.

2. Parametric modeling of hot plate welding

2.1. Finite element modeling of hot plate

According to the hot plate welding of the irregular workpiece, as shown in Figure 1(a), a portion of the hot plate was adopted to conduct the numerical calculation for optimization of the temperature uniformity on the faying surfaces used for hot plate welding. The three-dimensional finite element model with the length of 480 mm, the width of 150 mm and the height of 150 mm was established to carry out the heat transfer analysis of hot plate welding, as shown in Figure 1(b). The faying surface used for welding of plastic components is on the upper surface of the hot plate model. The distance between the faying surface and the upper surface of hot plate is 10mm, and the widths of the faying surface along the X-axial and Z-axial directions are 40mm and 20mm, respectively. Through the trial calculations, the C3D8T elements with the size of 10mm were utilized to mesh the there-dimensional finite element model, and the four element layers in the distance between the faying surface and the upper surface of the hot plate were adopted for calculating the temperature gradient, as shown in Figure 1(c). The 6061 aluminum alloy was used as the material of hot plate, the mass density is $2800\mathrm{kg/m^3}$, the specific heat capacity is $896\mathrm{J/(kg \cdot K)}$, and the thermal conductivity is $155\mathrm{W/(m \cdot K)}$.

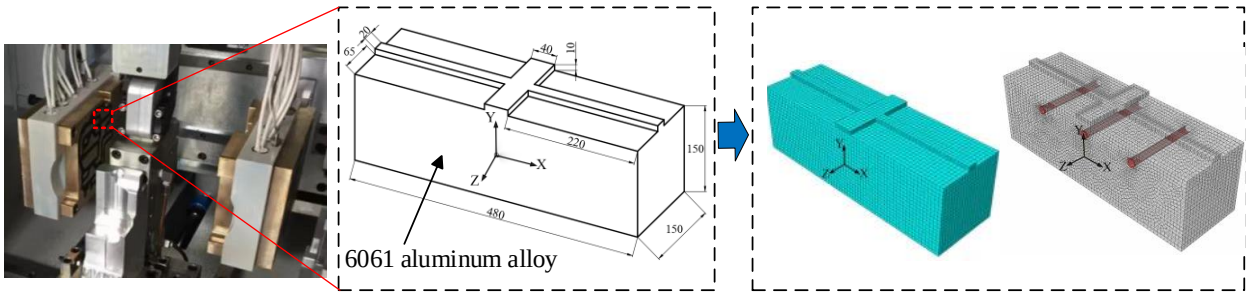

(a) (b) (c)

Figure 1. Three-dimensional finite element model of hot plate: (a) hot plate welding machine, (b) geometric dimensions, (c) finite element model.

Considering the stable temperature field produced by hot plate welding is the optimization objective, and the process of achieving the stable temperature field is not taken into consideration in this work, therefore the numerical calculation method for the steady-state heat transfer was employed to simulate the temperature field resulting from thermal conduction of hot plate for reducing the computation cost.

Three parallel heating holes with the diameter of 15mm were perforated in the XOY plane along the Z-axial direction according to experience, as shown in Figure 1(c). The heating rods were inserted into the heating holes for the thermal conduction of hot plate welding. For the sake of simplicity, the heat transfer by contact between the outer surfaces of the heating rods and the inner surfaces of the heating holes was simplified to applying the heat fluxes to the inner surfaces of the heating holes directly. The relationship between the power of the heating rod and the heat flux applying to the inter surface of heating

hole is calculated as

$$q = \frac{P}{\pi dL} \tag{1}$$

where P is the power of the heating rod, q is the heat flux applying to the inter surface of heating hole, d and L are the diameter and length of the heating rod, respectively. The initial temperature of the hot plate is 30°C, and the objective temperature required for hot plate welding is 200°C. The convective heat transfer between the outer surface of the hot plate and air was conducted by setting the convective heat transfer coefficient, which is $20\mathrm{W}/(\mathrm{m}^2 \cdot \mathrm{K})$ at the room temperature. The heat transfer resulting from thermal radiation of the heating rod was not taken into consideration in this work.

2.2. FEM-GA coupled optimization framework

To find the optimal positions of heating holes and the heat fluxes applying to the heating holes for improving the temperature uniformity of hot plate welding, the FEM-GA coupled parametric modeling and computation were conducted through the secondary development of FEM software, as shown in Figure 2. The positions of heating holes and the heat fluxes applying to the heating holes are the variables to be optimized and the minimum temperature difference on the faying surface used for hot plate welding is the optimizing objective. Based on the coordinates of the centers of the heating holes and the heat fluxes obtained by GA calculation, the parametric modeling of hot plate is carried out through Python interface provided by ABAQUS/CAE. The steady-state heat transfer is adopted to calculate the temperature field on the faying surface used for hot plate welding, and the FEM-calculated temperatures are fed back to GA for calculating the fitness values. If the GA-calculated fitness value has not reached the stability level, the newly generated coordinates of the centers of the heating holes and the heat fluxes by the selection, crossover and mutation of GA are then used to re-conduct the parametric modeling of hot plate and the finite element calculation of steady-state heat transfer.

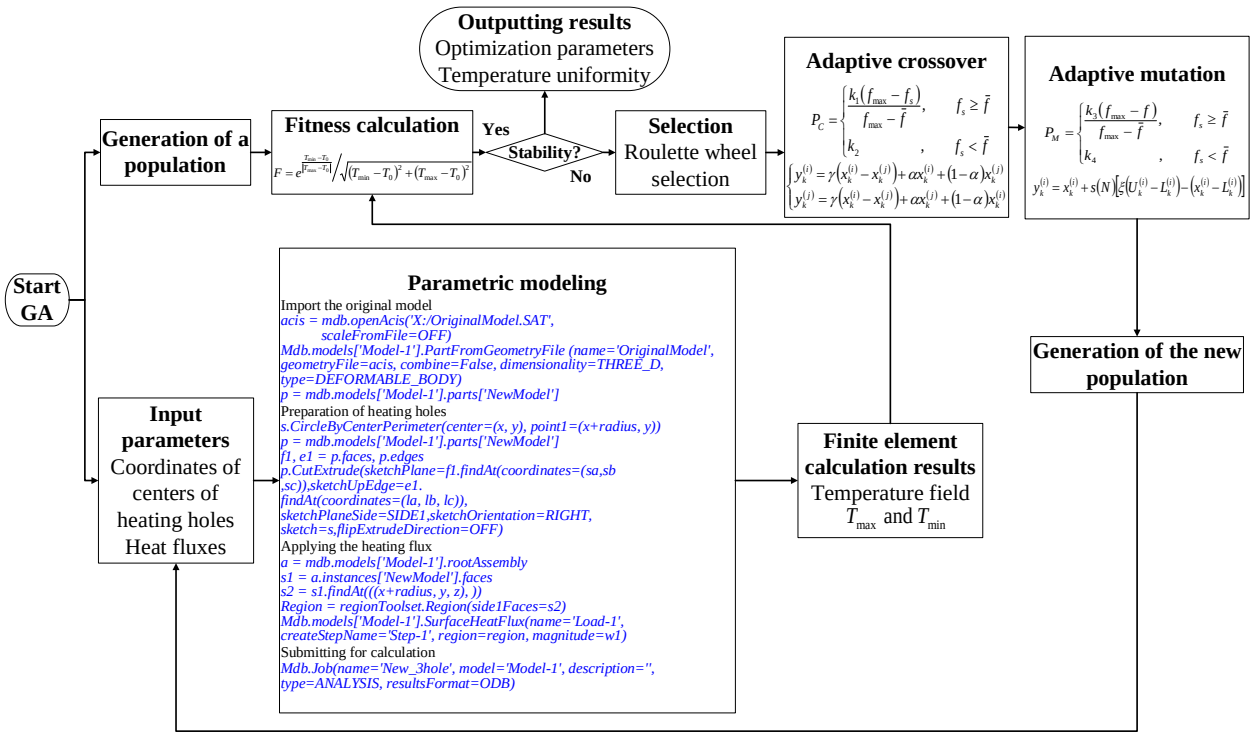

Figure 2. FEM-GA coupling optimization framework

In order to optimize the temperature uniformity of hot plate welding more quickly and effectively, the novel GA was developed in this work. There are thirty individualities in the population for a generation. In the process of the population evolution, the adaptive crossover probability (P_C) and adaptive mutation probability (P_M) were developed and are respectively expressed as [24]

$$P_C = \begin{cases} \dfrac{k_1(f_{max} - f_s)}{f_{max} - \bar{f}}, & f_s \geq \bar{f} \\ k_2 \quad , & f_s < \bar{f} \end{cases} \tag{2}$$

$$P_M = \begin{cases} \dfrac{k_3(f_{max} - f)}{f_{max} - \bar{f}}, & f \geq \bar{f} \\ k_4 \quad , & f < \bar{f} \end{cases} \tag{3}$$

where, f_{max} is the maximum fitness value among the 30 individualities of a generation; $\bar{f}$ is the averaged fitness value in the population; f_s is the larger fitness value of the two individualities to cross; f is the fitness value of the selected mutation individual; k_1, k_2, k_3 and k_4 are four constants and $k_1 = k_3 = 1$, $k_2 = k_4 = 0.5$ in the present work. In Eq. (2) and Eq. (3), the denominator $(f_{max} - \bar{f})$ is responsible for the increase of population diversity, and the numerator $(f_{max} - f_s)$ or $(f_{max} - f)$ is conductive to preserving the excellent individuals.

The fitness value is defined as

$$F = \frac{e^{\frac{T_{min} - T_0}{|T_{max} - T_0|}}}{\sqrt{(T_{min} - T_0)^2 + (T_{max} - T_0)^2}} \tag{4}$$

where, T_0 is the target temperature, $T_0 = 200°C$; T_{max} and T_{min} are the maximum and minimum values in the temperature field on the faying surface produced by hot plate welding, respectively. According to Eq. (4), the larger the fitness value is, the more uniform the temperature field of the hot plate welding becomes.

In the process of crossover operation, coding with real number is adopted. Assuming that the two-parent chromosomes selected for crossover are $x^{(i)} = \left\{x_1^{(i)}, x_2^{(i)}, \cdots, x_N^{(i)}\right\}$ and $x^{(j)} = \left\{x_1^{(j)}, x_2^{(j)}, \cdots, x_N^{(j)}\right\}$, in which $i, j = 1, 2, \cdots, 30$ represent the *i*th and *j*th parent chromosomes, *N* is the number of the optimization variable, the accordingly generated two-offspring chromosomes are determined as

$$\begin{cases} y_k^{(i)} = \gamma\left(x_k^{(i)} - x_k^{(j)}\right) + \alpha x_k^{(i)} + (1 - \alpha)x_k^{(j)} \\ y_k^{(j)} = \gamma\left(x_k^{(i)} - x_k^{(j)}\right) + \alpha x_k^{(j)} + (1 - \alpha)x_k^{(i)} \end{cases} \tag{5}$$

where, $k = 1, 2, \cdots, N$; $x_k^{(i)} \in x^{(i)}$, $x_k^{(j)} \in x^{(j)}$, $y_k^{(i)} \in y^{(i)}$, $y_k^{(j)} \in y^{(j)}$; $\alpha = 0.6$ in this work; γ is a random value in the range from 0 to 1, which is applied to improve the algorithm search space greatly, at the same time avoiding GA being easy to fall into the partial minimum flaw.

In the process of mutation operation, the single-point mutation is adopted. If $x_k^{(i)}$ ($x_k^{(i)} \in x^{(i)}$) is selected to mutate and $x_k^{(i)}$ is in the range of $\left(L_k^{(i)}, U_k^{(i)}\right)$ in which $L_k^{(i)}$ and $U_k^{(i)}$ respectively represent the lower and upper in the range of optimization parameters, then the mutated one ($y_k^{(i)}$) from $x_k^{(i)}$ is in the range of Ω that is expressed as

$$\begin{cases} \Omega = \left\{ x_k^{(i)} - s(N) \cdot \left(x_k^{(i)} - L_k^{(i)} \right),\ x_k^{(i)} + s(N) \cdot \left(U_k^{(i)} - x_k^{(i)} \right) \right\} \\ s(N) = 1 - r^{\left(1 - \frac{N}{N_{\max}}\right)^b} \\ y_k^{(i)} = x_k^{(i)} - s(N) \cdot \left(x_k^{(i)} - L_k^{(i)} \right) + \xi \cdot s(N) \cdot \left(U_k^{(i)} - L_k^{(i)} \right) \\ y_k^{(i)} \in \Omega \end{cases} \tag{6}$$

where, $s(N)$ is used to regulate the global search ability of GA; N is the iteration number; N_{max} represents the maximum iteration number; ξ is a random value in the range from 0 to 1; r and b are two constants, $r = 0.2$ and $b = 3$ obtained by trial and error method in this work. In the case of the smaller value of N, Ω becomes larger. As a result, the mutation would become more significant. On the other hand, as N increases, Ω becomes smaller and smaller, thereby the search speed of GA is improved significantly.

3. FEM-GA coupling optimization results

In order to improve the temperature uniformity on the faying surface used for hot plate welding, under the FEM-GA coupling optimization framework, two optimal design methods were proposed in this work. (1) Two-stage sequent optimal design method, two analysis steps are set up for the sequential optimization of the heat fluxes applying to the heating holes and positions of the heating holes. (2) Simultaneous optimal design method, both the heat fluxes and positions of the heating holes are optimized simultaneously.

3.1. Two-stage sequent optimal design method

With respect to the two-stage sequent optimization, the FEM-GA coupling calculation for improving the temperature uniformity of hot plate welding is conducted by setting two analysis steps, and the two-stage sequent optimization scheme is presented in Figure 3.

The first analysis step is used to optimize the heat fluxes applying to the heating holes, assuming that the positions of the heating holes are fixed. Three heating holes with the diameter of 15 mm are regularly perforated in the XOY surface along the Z-axial direction of the hot plate model, as shown in Figure 3. According to experiences, the distance between the centers of three heating holes and the upper surface of the hot plate model is 27.5 mm, and the distance between the center of the heating hole and the side of the hot plate model is equal to the distance of the adjacent heating holes centers, which is 120 mm. With the FEM-GA coupling optimization framework, the heat fluxes of heating rods inside the three heating holes are optimized in the range from 10kw/m^2 to $80\text{kw/}m^2$. As seen in Figure 3, for the heat flux of the heating rod inside the heating hole 1 that is represented by H1, the optimized heat fluxes of the 30 individuals are mostly concentrated in the $41\text{kW/}m^2$. Due to the symmetry of the heating hole 2 (H2) and heating hole 3 (H3), both the optimized heat fluxes of the heating rods inside H2 and H3 are mostly concentrated in the $64\text{kW/}m^2$, which are larger than the heat flux of the heating rod inside H1.

The second analysis step is used to optimize the positions of the three heating holes, assuming that the heat fluxes applying to the three heating holes are the same. The constant heat flux ($56.55\text{kW/}m^2$) with the averaged value of the previously-optimized heat fluxes applying to the three heating holes of H1 ($41.23\text{kW/}m^2$), H2 ($64.21\text{kW/}m^2$) and H3 ($64.20\text{kW/}m^2$), is used as the constant heat sources to optimize the positions of the three heating holes. The optimization range of the positions of the heating

holes are (-240 mm, 240 mm) for the X coordinates and (-50 mm, 50 mm) for the Y coordinates. As seen in Figure 3, different from the three regularly-perforated heating holes, the distances from the three centers of the Step2-optimized heating holes to the upper surface of the hot plate model are not the same. The distance between the Step2-optimized H2 and the upper surface of the hot plate model is the largest (127.61 mm), whereas the distance between the Step2-optimized H3 and the upper surface of the hot plate model is the smallest (121.78 mm). The distance between Step2-optimized H2 and H1 is approximately equal to the distance between H3 and H1.

To sum up, with the FEM-GA coupling optimization method, the two-stage sequent optimization results of the heat fluxes applying to the heating holes and the positions of the heating holes are described in the form of (heat flux, X-coordinate, Y-coordinate), yield: H1(41.23kW/m^2, 3.23mm, -39.73mm), H2(64.21kW/m^2, -195.0mm, -42.61mm), H3(64.20kW/m^2, 182.68mm, -36.78mm).

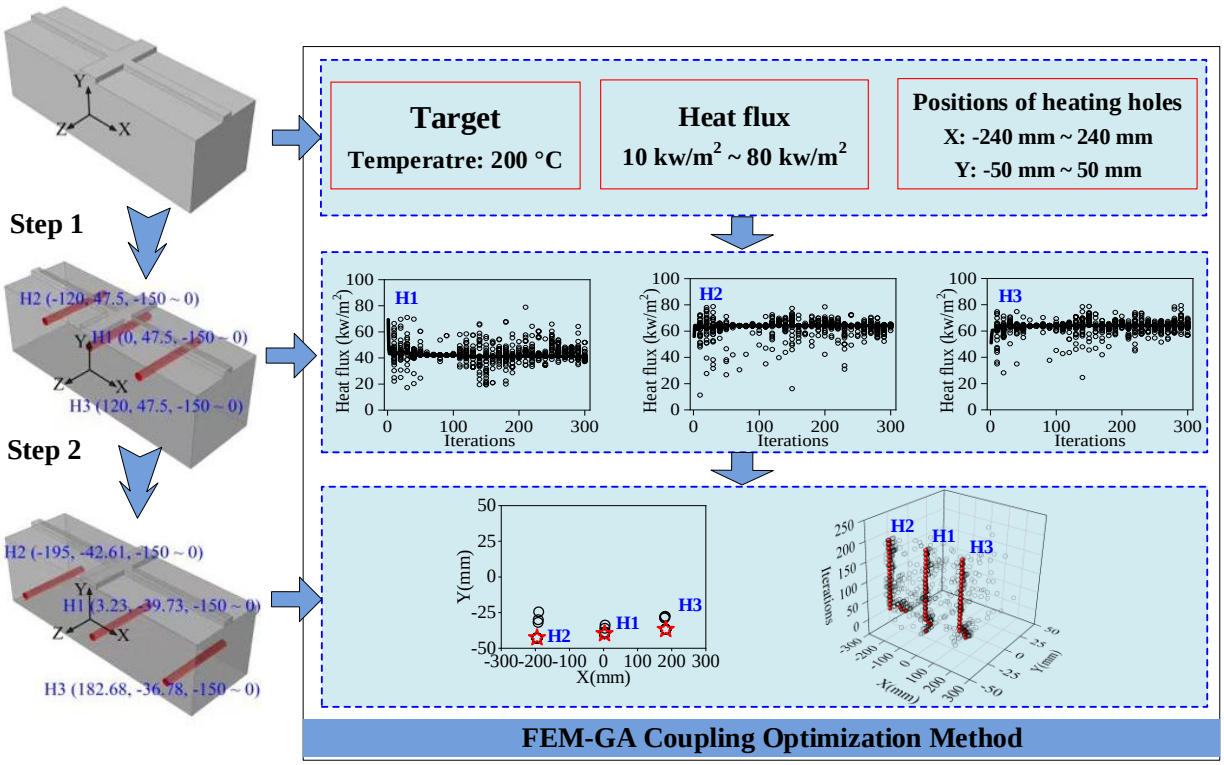

Figure 3. FEM-GA coupling two-stage sequent optimal design method

Figure 4(a) shows the GA-calculated fitness values used for describing the temperature uniformity on the faying surface with regard to the two analysis steps. For the first analysis step, when the iterations exceed 111, the fitness value is stable at 0.107. On the other hand, for the second analysis step, when the iterations exceed 56, the fitness value is stable at 1.017. As well known, the larger the fitness value is, the better optimization effect is. In addition, the number of the iterations used to obtain the stable fitness value in the second analysis step is significantly smaller than that in the first analysis step. Therefore, it takes a large number of iterations to optimize the heat fluxes applying to the heating holes based on the assumed positions of the three heating holes, but the temperature uniformity depending on the optimized heat fluxes is not desirable. In other words, compared to the optimization of the heat fluxes applying to the heating holes located at the experience-based positions, the optimization of the positions of the heating holes subjecting to the same heat flux would be more conducive to improving the temperature uniformity on the faying surfaces produced by the hot plate welding.

Figure 4(b) presents the FEM-GA coupling optimization results of the temperature uniformity on

the faying surfaces produced by hot plate welding in the first analysis step. As seen from Figure 4(b), with the increase of iterations, the temperature difference between the maximum and minimum temperatures on the faying surface is mainly concentrated at 9.5°C. Figure 4(b) exhibits the temperature field on the faying surface resulting from the optimized heat fluxes. The higher temperature on the faying surfaces is at the position with the smaller distance from the heating holes, which accords well with the natural law of heat conduction. As shown in Figure 4(b), the largest value of temperature difference on the faying surface is 9.4°C, which is in good accordance with the GA optimization results in Figure 4(b).

On the other hand, make use of the averaged value of the Step1-optimized heat fluxes as the constant heat flux to optimize the positions of the heating holes to achieve the excellent temperature uniformity of hot plate welding. As the number of iterations increases, the minimum temperature difference of the 30 individuals resulting from FEM-GA coupling optimization approaches 1.0°C, as shown in Figure 4(c), which is significantly smaller than the minimum temperature difference in the case of optimization of the heat fluxes at the fixed heating holes. Figure 4(c) presents the temperature field on the faying surface in the case of the three optimized the positions of the three heating holes. Similar to Figure 4(b), the larger temperature is at the position with the smaller distance from the heating holes. However, different from Figure 4(b), due to the different distances between the heating holes and the faying surface, the asymmetrical distribution of the temperature can be seen in Figure 4(c). Therefore, it is demonstrated that the two-stage sequent optimization method is able to effectively improve the temperature uniformity on the faying surface by optimizing the heat fluxes at the fixed heating holes firstly and then optimizing the positions of the heating holes associated with the constant heat flux sequentially, as shown in Figure 3.

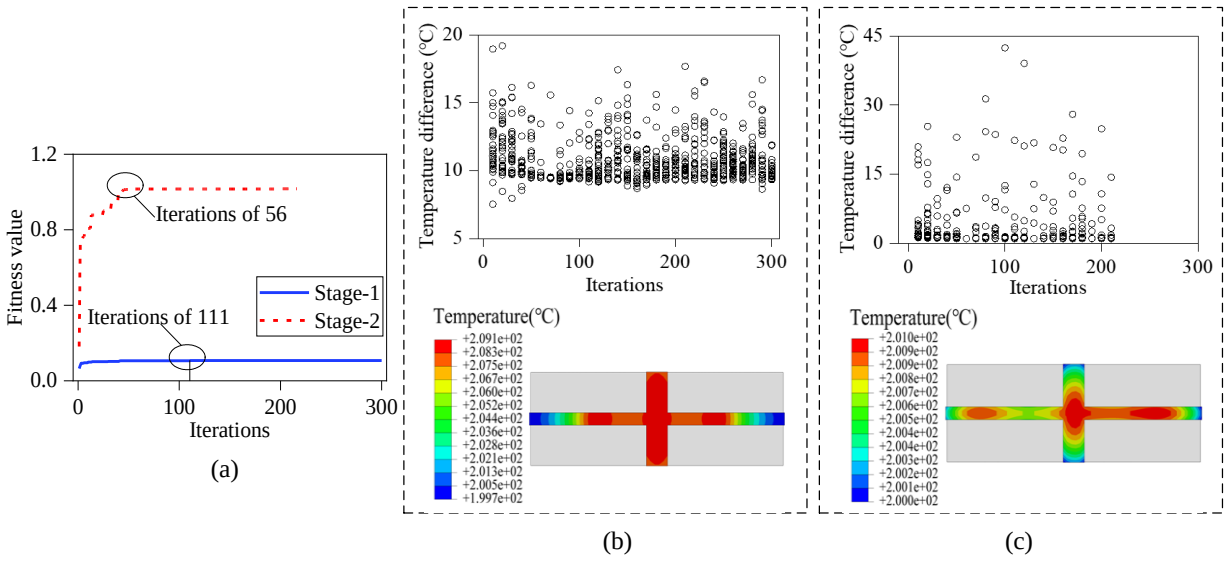

Figure 4. FEM-GA coupling two-stage sequent optimization results: (a) GA-calculated fitness values of temperature uniformity, (b) the first step used in the two-stage sequent optimization, (c) the second step used in the two-stage sequent optimization.

3.2. Simultaneous optimal design method

Under the FEM-GA coupling optimization framework, taking both the positions of the heating holes and heat fluxes applying to the heating holes as the optimization variables, an attempt to develop the simultaneous optimal design method is made for improving the temperature uniformity on the faying

surfaces used for hot plate welding as much as possible. Figure 5 presents the calculation framework of the FEM-GA coupling simultaneous optimization. Different from the two-stage sequent optimization scheme, there is only one analysis step used for finding the optimal heat fluxes and positions of the three heating holes. With respect to the same input parameters ($q \in (10\text{kw}/m^2,\ 80\text{kw}/m^2)$), $X \in (-240\text{mm}, 240\text{mm})$, $Y \in (-50\text{mm}, 50\text{mm})$, where q represents the heat flux, X and Y represent the X and Y coordinates, respectively), comparing with the results of the two-stage sequent optimization, the simultaneous optimization method presents the better convergence. As shown in Figure 5, the optimized heat fluxes are mostly concentrated at $30\text{kW}/m^2$, $62\text{kW}/m^2$ and $76\text{kW}/m^2$applying to the heating holes H1, H2 and H3, respectively. On the other hand, the positions of the three heating holes are optimized at H1(-30.85 mm, 40.03 mm, 0), H2(-181.87 mm, -20.53 mm, 0) and H3(150.7 mm, -7.9 mm, 0), respectively.

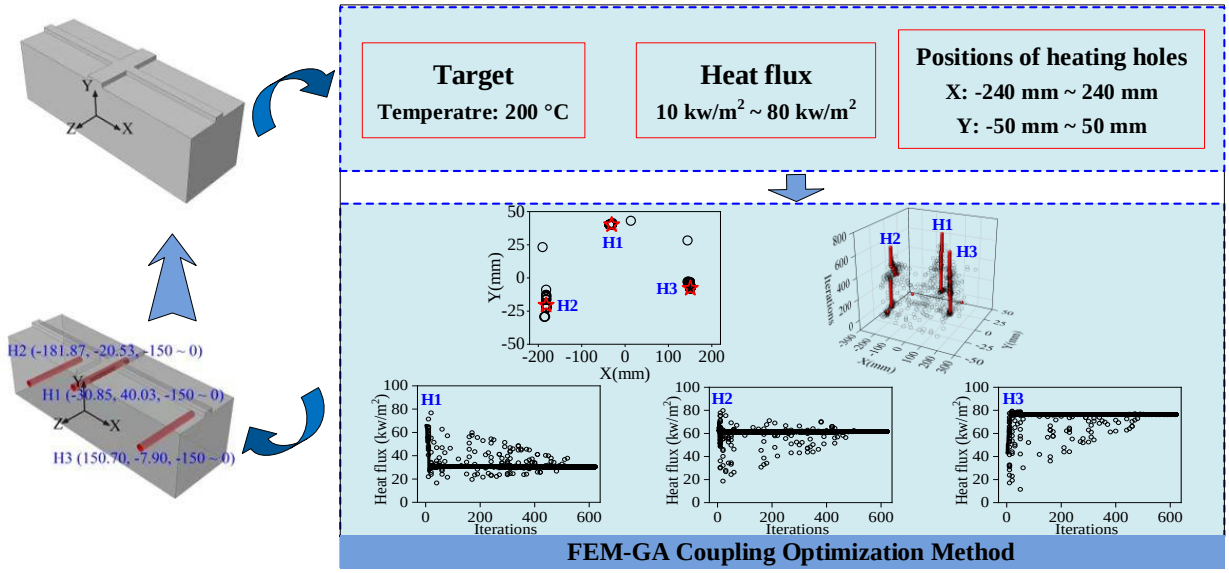

Figure 5. FEM-GA coupling simultaneous optimal design method

Figure 6(a) shows the evolution of the fitness value resulting from FEM-GA coupling calculation. With the increase of iterations, the GA-calculated fitness value increases rapidly at first and then gradually tends to be stable. The maximum fitness value is 0.561 and is significantly smaller than the two-stage sequent optimization result, it reveals that the simultaneous optimization effects are not as good as the two-stage sequent optimization effects. As shown in Figure 6(b), the minimum value of temperature difference of the 30 individuals remains fairly constant. In particular, when the number of iterations exceeds 500, the temperature differences of the 30 individuals are almost in consistent. The finally optimized temperature field produced by the hot plate welding is presented in Figure 6(c). The minimum temperature difference on the faying surface produced by the hot plate welding is 1.8°C, which is roughly 2 times of the minimum temperature difference resulting from the two-stage sequent optimization.

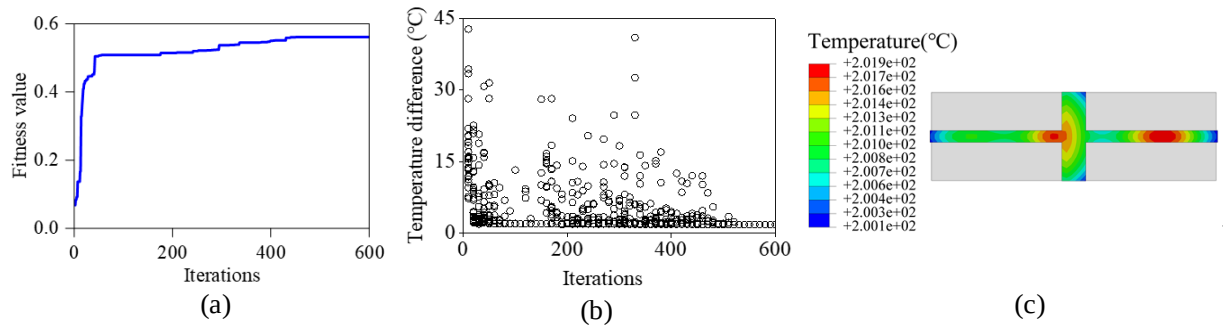

Figure 6. The simultaneous optimization results: (a) GA-calculated fitness values, (b) distribution of temperature difference, (c) temperature field on the faying surface.

With the two-stage sequent optimal design method and the simultaneous optimal design method, the optimization results of the heat fluxes and positions of the three heating holes are presented in Figure 7. As seen in Figure 7(a), since the H1 is located in the middle of H2 and H3, the optimized heat flux at H1 is smaller than that at H2 and H3. With the two-stage sequent optimal design method, the heat flux applying to H2 is approximately equal to the heat flux applying to H3, whereas the simultaneously-optimized heat flux applying to H2 is smaller than that applying to H3. In addition, with respect to H1, the sequentially-optimized heat flux is larger than that obtained by the simultaneous optimization method. With regard to H1 (or H2, H3), the difference in the optimized heat fluxes by the two-stage sequent optimal design method and the simultaneous optimal design method is related to the optimized positions of H1 (or H2, H3), as shown in Figure 7(b). For H1, H2 and H3, the simultaneously-optimized Y-coordinates are all larger than that obtained by the two-stage sequent optimal design method. Especially for H1, the sequentially-optimized position is closed to the bottom surface of the hot plate model, whereas the H1 position optimized by the simultaneous optimal design method is adjacent to upper surface of the hot plate model, the distance along Y-axial direction between the two optimized positions of H1 resulting from the two optimal design methods is about 80 mm. As well known, the larger the distance between the heating holes and the faying surface is, the more uniform the temperature field on the faying surface becomes.

Figure 7(c) compares the computation efficiency and optimization results of the two-stage sequent optimization and simultaneous optimization. The computation efficiency is represented by the iteration number, and the optimization results are represented by the minimum temperature difference on the faying surface. As seen in Figure 7(c), with the two-stage sequent optimal design method, after 167 (56+111) iterations, the minimum temperature difference on the faying surface is 1.0°C, whereas the simultaneously-optimized minimum temperature difference is 1.8°C after 451 iterations. Therefore, based on the FEM-GA coupling calculation framework, the two-stage sequent optimal design method has the higher efficiency and ability in optimizing the temperature uniformity used for hot plate welding, in comparison to the simultaneous optimal design method. However, it should be noted that the regularly-distributed heating holes according to experience are significant for the two-stage sequent optimal design method to optimize the heat fluxes applying to the heating holes. However, there are no any preparation needs to complete ahead of schedule for the simultaneous optimal design method.

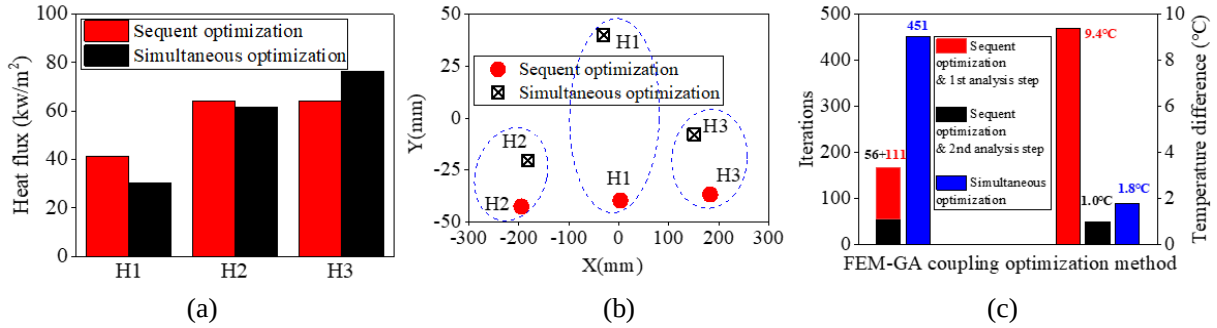

Figure 7. Comparison of the optimized heat fluxes and positions of the three heating holes by using the two-stage sequent optimal design method and simultaneous optimal design method: (a) heat fluxes applying onto the three heating holes, (b) positions of the three heating holes, (c) computation efficiency and the minimum temperature.

3.3. Optimization of orthogonal heating holes

As well known, the hot plate associated with the orthogonal heating holes are frequently used in the practical welding applications. With the simultaneous optimal design method, the temperature uniformity of hot plate welding in the case of the orthogonal heating holes was numerically optimized by the developed FEM-GA coupling calculation framework. In comparison to the parallel heating holes as described in the section of '*3.2 Simultaneous optimal design method*', besides the three parallel heating holes along the Z-axial direction, two parallel heating holes along the X-axial direction are added in the hot plate model. Therefore, there are five heating fluxes, three coordinates (X, Y) of the heating holes center in the XOY plane and two coordinates (Y, Z) of the heating holes center in the YOZ plane, as shown in Figure 8.

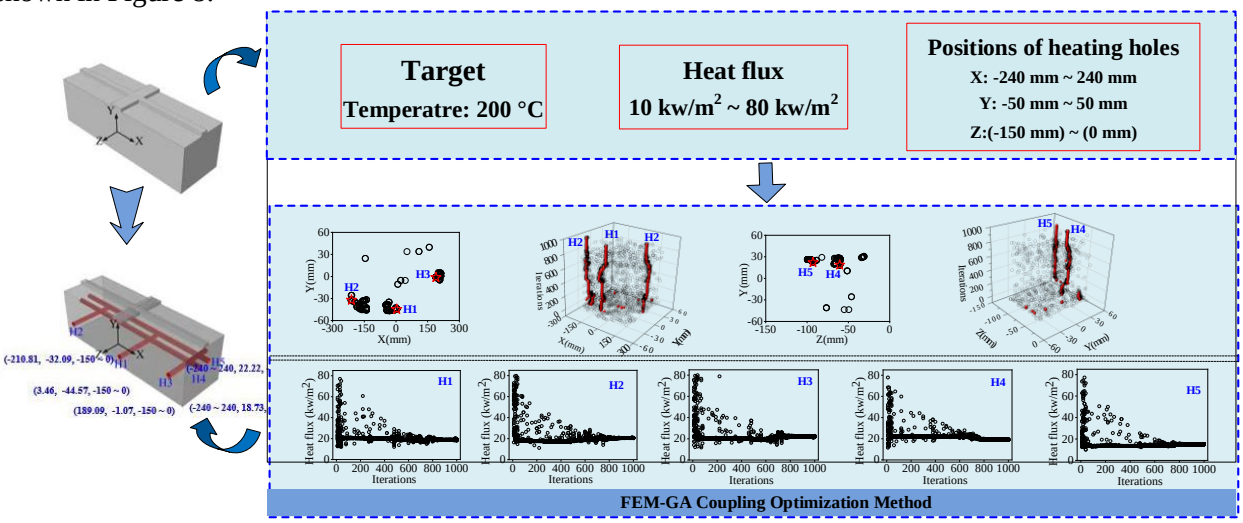

Figure 8. FEM-GA coupling optimization in the case of the orthogonal heating hole

Figure 8 presents the calculation framework of FEM-GA coupling optimization for improving the temperature uniformity of hot plate welding in the case of the orthogonal heating holes. The input parameters and target temperature are the same as the calculation framework used in the hot plate model associated with the parallel heating holes. As seen from Figure 8, due to the increase of the heating holes,

the simultaneously-optimized heat fluxes at the five heating holes are around $20\text{kW}/m^2$ that is smaller than the heat fluxes in the cases of the two-stage sequent optimization and simultaneous optimization, revealing that the orthogonal heating holes can effectively reduce the heat flux at each heating hole. On the other hand, the positions of the heating holes are almost symmetrical in the X-axial and Z-axial directions, and the Y-axial coordinates of H4 and H5 heating holes are almost the same, whereas the Y-axial coordinate of H3 heating hole is larger than that of H2 heating hole, indicating that the distance between the position of H3 heating hole and the faying surface is smaller than the distance between the position of H2 heating hole and the faying surface.

Figure 9(a) presents the evolution of fitness value with the increase of iterations in the case of the orthogonal heating holes. The number of iterations for obtaining the maximum fitness value is approximately 800 that is significantly larger than the iteration numbers corresponding to the maximum fitness value in the case of three parallel heating holes, which is attributed to the increase of the optimization variables as a result of the increase of the heating holes. As shown in Figure 9(b), the minimum temperature difference of the 30 individuals is stable at 1.3°C when the iteration numbers exceed 800. Figure 9(c) exhibits the optimized temperature field on the faying surface produced by the hot plate welding. In comparison to the optimized temperature fields resulting from the three parallel heating holes, the optimized temperature field in the case of the orthogonal heating holes presents the good mirror symmetry, and the more uniform temperature field can be obtained on the faying surface along the X-axial direction.

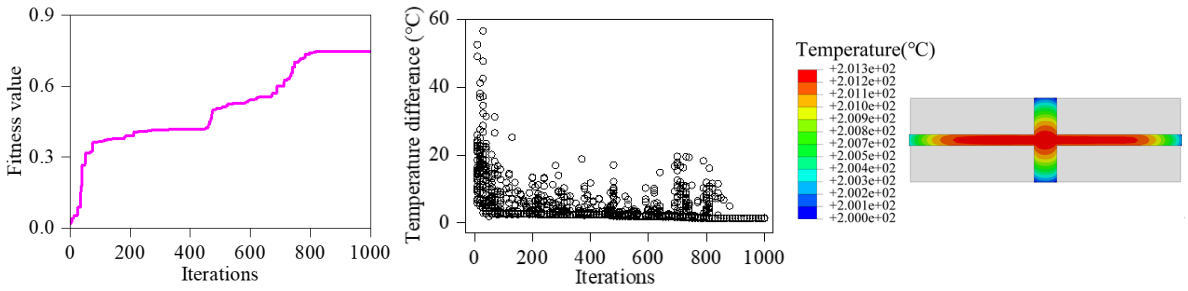

(a) (b) (c)

Figure 9. The optimization results in the case of the orthogonal heating holes: (a) GA-calculated fitness values of temperature uniformity, (b) distribution of temperature difference, (c) temperature field on the faying surface.

4. Conclusions

In order to improve the temperature uniformity on the faying surface used for hot plate welding, two FEM-GA coupling optimal design methods, including the two-stage sequent optimal design method and the simultaneous optimal design method, were developed and completed through secondary development of FEM software, respectively. The obtained conclusions are drawn as follows:

With the two-stage sequent optimal design method, in the case of the experience-based parameters initialization, the temperature difference on the faying surface is stable at 1.0°C after 167 iterations; whereas the temperature difference of 1.8°C on the faying surface can be obtained by the simultaneous optimal design method within 451 iterations.

The optimal parameters including the positions of the heating holes and the heat fluxes applying to the heating holes resulting from the two-stage sequent optimal design method are different from the results of the simultaneous optimization, especially for the positions of the heating holes.

In the case of the hot plate associated with the orthogonal heating holes, the temperature difference on the faying surface can reduce to 1.3 °C by using the simultaneous optimal design method. However, it requires 800 iterations due to the increase in the optimization parameters.

Funding

The authors are grateful for the Open Fund of Collaborative Innovation Center of High-end Laser Manufacturing Equipment Co-sponsored by Ministry and Province (JGKF-202202), and Graduate Innovation and Entrepreneurship Project of Anhui University of Science and Technology (2023CX2078, 2023200598).

Nomenclature

Variable or parameter	
P	The power of the heating rod [W]
q	The heat flux applying to the inter surface of heating hole [$\mathrm{W}/\left(\mathrm{m}^2\cdot\mathrm{K}\right)$]
d	Diameter of the heating rod [mm]
L	Length of the heating rod [mm]
P_C	Adaptive crossover probability of GA [-]
P_M	Adaptive mutation probability of GA [-]
f_{max}	Maximum fitness value among the individualities of a generation [-]
$\bar{f}$	Averaged fitness value in the population [-]
f_s	Larger fitness value of the two individualities to cross [-]
f	Fitness value of the selected mutation individual [-]
T_0	Target temperature in the temperature field on the faying surface produced by hot plate welding [$^{\circ}\mathrm{C}$]
T_{max}	Maximum values in the temperature field on the faying surface produced by hot plate welding [$^{\circ}\mathrm{C}$]
T_{min}	Minimum values in the temperature field on the faying surface produced by hot plate welding [$^{\circ}\mathrm{C}$]
N	The number of the optimization variable [-]
N_{max}	Represents the maximum iteration number [-]
Greek letters	
Ω	Mutation interval of GA [-]
ξ	Random value [-]

References

1. Yawen, O., Chao, C., Research Advances in the Mechanical Joining Process for Fiber Reinforced Plastic Composites, *Composite Structures*, 296(2022), pp. 115906
2. Kwon, D.J., *et al*., Enhanced Mechanical Joining between Carbon-Fiber-Reinforced Plastic and Steel Plates Using the Clearance-Filling Effect of Structural Adhesive, *Applied Sciences-Basel*, 13(2023), 7, pp. 4332
3. Tofil, S., *et al*., Surface Laser Micropatterning of Polyethylene (PE) to Increase the Shearing Strength of Adhesive Joints, *Lubricants*, 11(2023), 9, pp. 368

4. Ma, G., *et al*., Mechanical Performance of Adhesively Bonded Carbon Fiber Reinforced Boron-Modified Phenolic Resin Plastic- Titanium Single- Lap Joints at High Temperature, *Polymer Composites*, 45(2024), 1, pp. 777-791
5. Varga, J., *et al*., Quality Analysis of Bonded Joints in The Renovation of Plastic Automotive Parts, *Applied Sciences-Basel*, 14(2023), 1, pp. 217
6. Ülker, A., *et al*., Optimization of Welding Parameters of Hot Plate Welded PC/ABS Blends by Using the Taguchi Experimental Design Method, *Journal of Elastomers and Plastics*, 50 (2018), 2, pp. 162-181
7. Ülker, A., *et al*., Application of the Taguchi Method for the Optimization of the Strength of Polyamide 6 Composite Hot Plate Welds, *Materials Science and Technology*, 57(2015), 6, pp. 531-542
8. Wang, G., *et al*., Multi-Objective Optimization Design of The Heating/Cooling Channels of the Steam-Heating Rapid Thermal Response Mold Using Particle Swarm Optimization, *International Journal of Thermal Sciences*, 50(2011), 5, pp. 790-802
9. Chen, S.C., *et al*., Variable Mold Temperature to Improve Surface Quality of Microcellular Injection Molded Parts Using Induction Heating Technology, *Advances in Polymer Technology*, 27(2008), pp, 224-232
10. Chen, S.C., *et al*., Mold Temperature Control Using High-Frequency Proximity Effect Induced Heating, *International Communications in Heat and Mass Transfer*, 39(2012), 2, pp. 216-223
11. Lambiase, F., Genna, S., Homogenization of Temperature Distribution at Metal-Polymer Interface During Laser Direct Joining, *Optics and Laser Technology*, 128(2020), pp. 106226
12. Lambiase, F., *et al*., Optimization of Laser-Assisted Joining Through an Integrated Experimental-Simulation Approach, *International Journal of Advanced Manufacturing Technology*, 97(2018), (5-8), pp.2655-2666
13. Alperen, Y., Sertac, C., Multi Objective Optimization of a Micro-Channel Heat Sink Through Genetic Algorithm, *International Journal of Heat and Mass Transfer*, 146(2020), pp.118847
14. Novakovic, B., Kashkoush, M., Modeling the Matching Stage of HDPE Hot Plate Welding: A Study Using Regression and Support Vector Machine Models, *Polymer Engineering and Science*, 64(2024), 2, pp. 827-844.
15. Mathiyazhagan, K., *et al*., Modeling the Interrelationship Between the Parameters for Improving Weld Strength in Plastic Hot Plate Welding: A DEMATEL Approach, *Journal of Elastomers and Plastics*, 52(2020), 2, pp. 117-141
16. Krzysztof, W., *et al*., Experimental Approach to Modeling of the Plasticizing Operation in the Hot Plate Welding Process, *Archives of Civil and Mechanical Engineering*, 22 (2021), 1, pp. 16
17. Krzysztof, W., *et al*., Designing of the Electromechanical Drive for Automated Hot Plate Welder Using Load Optimization with Genetic Algorithm, *Materials*, 15(2022), 5, pp. 1787
18. Riahi, M., *et al*., Analysis of Effect of Pressure and Heat on Mechanical Characteristics of Butt Fusion Welding of Polyethylene Pipes, *Polymer - Plastics Technology and Engineering*, 50(2011), 9, pp. 907-915
19. Jiang, M., et al., Optimization of Micro-Channel Heat Sink Based on Genetic Algorithm and Back Propagation Neural Network, Thermal Science, 27(2023), 1A, pp. 179-193
20. Taheri, Y., et al., Multi-Objective Optimization of Three Rows of Film Cooling Holes by Genetic Algorithm, Thermal Science, 25(2021), 5A, pp.3531-3541
21. Corriveau, G., et al., Genetic Algorithms and Finite Element Coupling for Mechanical

Optimization, Advances in Engineering Software, 41(2010), 3, pp. 422-426
22. Kanssab, A., et al., Modeling and Optimization of Induction Cooking by the Use of Magneto-Thermal Finite Element Analysis and Genetic Algorithms, Frontiers of Electrical and Electronic Engineering, 7(2012), pp. 312-317
23. Ya, G., et al. Geometric Optimization for the Thermoelectric Generator with Variable Cross-Section Legs by Coupling Finite Element Method and Optimization Algorithm, Renewable Energy, (2022), pp.183294-303
24. Srinivas, M., Patnaik, M. L., et al., Adaptive Probabilities of Crossover and Mutation in Genetic Algorithms, IEEE Trans. Systems, Man, and Cybernetics, 24(1994), 4, pp. 656-667

Paper submitted: 12.11.2024
Paper revised: 25.11.2024
Paper accepted: 01.12.2024